

A “Naked” Fe^{III}-(O₂²⁻)-Cu^{II} Species Allows for Structural and Spectroscopic Tuning of Low-Spin Heme-Peroxo-Cu Complexes

Isaac Garcia-Bosch,[†] Suzanne M. Adam,[†] Andrew W. Schaefer,[‡] Savita K. Sharma,[†] Ryan L. Peterson,[†] Edward I. Solomon,^{*,‡} and Kenneth D. Karlin^{*,†}

[†]Johns Hopkins University, Baltimore, Maryland 21218, United States

[‡]Department of Chemistry, Stanford University, Stanford, California 94305, United States

Supporting Information

ABSTRACT: Here we describe a new approach for the generation of heme-peroxo-Cu compounds, using a “naked” complex synthon, [(F₈)Fe^{III}-(O₂²⁻)-Cu^{II}-(MeTHF)₃]⁺ (MeTHF = 2-methyltetrahydrofuran; F₈ = tetrakis(2,6-difluorophenyl)porphyrinate). Addition of varying ligands (L) for Cu allows the generation and spectroscopic characterization of a family of high- and low-spin Fe^{III}-(O₂²⁻)-Cu^{II}(L) complexes. These possess markedly varying Cu^{II} coordination geometries, leading to tunable Fe-O, O-O, and Cu-O bond strengths. DFT calculations accompanied by vibrational data correlations give detailed structural insights.

The interaction of transition metal ions with molecular oxygen (O₂) and its reduced derivatives, superoxide (O₂^{•-}), peroxide (O₂²⁻), or hydroperoxide (•OOH), and hydroxyl-radical (•OH) plays a critical role in oxidative processes.¹ For practical applications in the selective-efficient oxidation of organics or for fuel cell applications critical to future energy concerns and where O₂ may be electrocatalytically reduced to H₂O₂ or H₂O, first row transition metals such as Fe, Mn, or Cu are of great importance, having suitable redox behavior and low cost due to favorable earth abundance.² Fe and Cu are also utilized in biological systems, where “O₂ activation” occurs when metal-O₂ interactions lead to biological substrate oxidation (loss of H⁺ and e⁻) or oxygenation (with O atom insertion). The activation is reductive; reduced metals or other e⁻ sources promote formation of metal-bound reduced O₂ derivatives, as proposed to occur in Cu oxidase or heme peroxidase chemistry.^{3a} Our interest in such species is part of a goal to elucidate the underlying chemistry occurring at the active-site of heme-copper oxidases wherein a Cu center with a proximal heme effects 4e⁻/4H⁺ O₂-reduction to H₂O (Figure 1).^{3b} We wish to resolve the details of O₂-binding and O-O cleavage, as a function of heme-Cu proximity, Cu-ligation (donor numbers and type), and individual metal redox potentials, all with knowledge of previously established separate heme-O₂⁴ and Cu-O₂⁵ chemistries. The study of the kinetics-thermodynamics of key protonation and/or electron-transfer steps is also of utmost interest and importance,⁶ now within the confines of a coordination environment with heme *plus* Cu.

Because of the inherent instability of the putative intermediate species formed during the catalytic cycle of cytochrome *c* oxidase (CcO), we have long envisioned that a

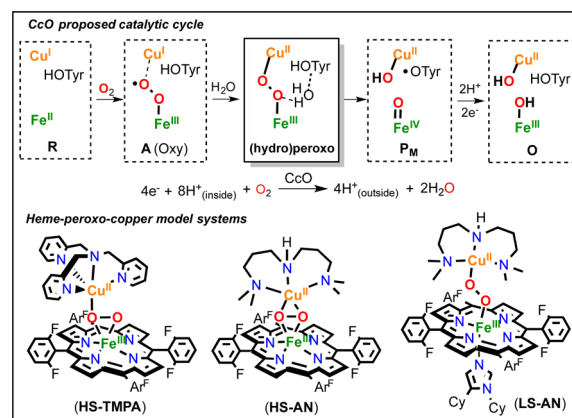


Figure 1. Proposed intermediates formed in the O₂-reduction catalyzed by CcO (top) and heme-(O₂²⁻)-Cu model complexes (bottom).

detailed study on the spectroscopic and chemical properties of model compounds is essential to understand the O-O cleavage step in these enzymes and to provide general insights into metal ion mediated O₂ reduction pathways. To this end and with a strategy involving a systematic ligand design and synthesis approach, we have developed a library of heme Fe^{II}-Cu^I O₂-adducts, leading to heme-(O₂²⁻)-Cu^{II} synthetic compounds possessing different peroxide binding modes (Figure 1, bottom).⁷⁻⁹

We characterized the high-spin (HS) species [(F₈)Fe^{III}-(O₂²⁻)-Cu^{II}(TMPA)]⁺, (HS-TMPA) (TMPA = tris((2-pyridyl)methyl)amine), formed via oxygenation of an (F₈)-Fe^{II}/[(TMPA)Cu^I]⁺ (1:1) mixture.^{8a} Spectroscopic and computational analyses led to its formulation as an Fe-(μ-η²:η¹-O₂²⁻)-Cu center (Figure 1).^{8b} Using the same strategy, addition of O₂ to an (F₈)Fe^{II}/[(AN)Cu^I]⁺ (1:1) mixture led to the formation of a HS [(F₈)Fe^{III}-(O₂²⁻)-Cu^{II}(AN)]⁺ complex, (HS-AN) (AN = bis(3-(dimethylamino)propyl)amine), in which the peroxo moiety was found to be bound in a side-on fashion (Figure 1).^{8c} A considerable advance came when we reported the generation of the low-spin (LS) analogue, [(DCHIm)(F₈)Fe^{III}-(O₂²⁻)-Cu^{II}(AN)]⁺, (LS-AN), by addition of an axial base (DCHIm = 1,5-dicyclohexylimidazole).^{9,10} The change in the spin state was associated with a change in the

Received: November 9, 2014

Published: January 16, 2015

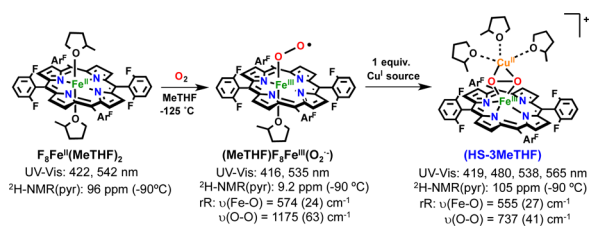


Figure 2. Sequential generation of $(MeTHF)F_8Fe^{III}(O_2^{\bullet-})$ and $(HS-3MeTHF)$ and their spectroscopic features. See the SI.

bridging mode of the peroxide to form an end-on $Fe^{III}-(\mu-\eta^1:\eta^1-O_2^{2-})-Cu^{II}$ center (Figure 1). Here we describe a stepwise strategy allowing for the synthesis of new kinds of heme- $(O_2^{2-})-Cu$ compounds by employing a new synthon, the solvato “naked” complex $[(F_8)Fe^{III}-(O_2^{2-})-Cu^{II}(MeTHF)_3]^+$, $(HS-3MeTHF)$. Simple addition of ligands of different denticity, such as TMPA and/or the unidentate DCHIm donor, leads to the formation of an array of HS/LS complexes.

Bubbling O_2 through a cold solution of F_8Fe^{II} in MeTHF (from -90 to -125 °C) resulted in the formation of $(MeTHF)F_8Fe^{III}(O_2^{\bullet-})$, having spectroscopic features (UV/vis, 2H NMR, resonance Raman (rR); Figure 2) identical to those observed for the close analogue $(THF)F_8Fe^{III}(O_2^{\bullet-})$.^{11,12} Addition of 1 equiv of $Cu^I(CH_3CN)_4(B(C_6F_5)_4)$ to this superoxo compound, monitored by UV/vis, led to the formation of a peroxo compound, $(HS-3MeTHF)$, with a UV/vis spectrum (Figure 3, blue spectrum) similar to that of other well-characterized bridging side-on $Fe-(\mu-\eta^2:\eta^2-O_2^{2-})-Cu$ complexes.^{7,12} The generation of $(HS-3MeTHF)$ was carried out via titration, adding 0.33–4 equiv of $Cu^I(CH_3CN)_4(B(C_6F_5)_4)$. The conversion exhibited isobestic behavior, showing a maximum formation for $(HS-3MeTHF)$ at 1 equiv of Cu(I) source, confirming the formulation of the HS peroxo complex as a 1:1 heme/Cu compound (see Supporting Information (SI)). Further characterization of $(HS-3MeTHF)$ was provided by 2H NMR spectroscopy. A pyrrole signal appeared in the paramagnetic region (105 ppm at -90 °C), which based on extensive precedent is suggestive of a complex with overall $S = 2$ spin state, derived from antiferromagnetic coupling of HS $Fe(III)$ ($S = 5/2$) and Cu(II) ($S = 1/2$) centers (see SI).¹² Additional proof was obtained by rR spectroscopy (Figure 3). One isotope-sensitive peak was observed at 737 cm^{-1} , which shifted to 696 cm^{-1} ($\Delta(^{18}O_2) = 41$ cm^{-1}) when $(HS-3MeTHF)$ was generated using $^{18}O_2$. This peak is assigned as an intraperoxide stretch of a side-on bridging peroxide, based on its low frequency and similarity to the other well-characterized side-on $Fe-(O_2^{2-})-Cu$ species.¹³ Another isotope-sensitive peak, corresponding to the Fe-O symmetric stretch, is overlapped by the analogous mode in $(MeTHF)F_8Fe^{III}(O_2^{\bullet-})$ present as a minor component in the sample, but spectral subtraction provided a peak position estimate of 555 cm^{-1} ($\Delta = 27$ cm^{-1}).^{14a}

Addition of 1 equiv of TMPA to $(HS-3MeTHF)$ resulted in the formation of the HS complex $(HS-TMPA)$, which was characterized by UV/vis, 2H NMR, and rR spectroscopies (Figure 3) and shown to be equivalent to this complex prepared directly earlier.⁸ This experiment provided proof of concept that the “naked” compound $(HS-3MeTHF)$ can be used as a synthon for the generation of many heme- $(O_2^{2-})-Cu$ compounds. Addition of 1 equiv of DCHIm to $(HS-TMPA)$ caused a change in the UV/vis features, in both the Q-band and lower-energy regions, suggesting the formation of the LS

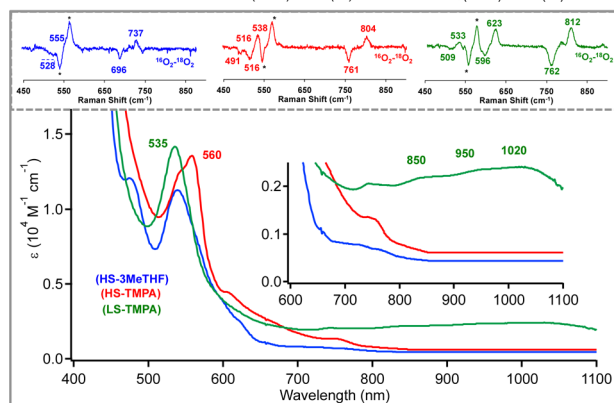
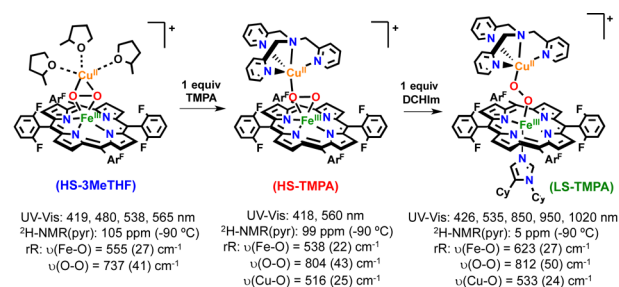


Figure 3. Sequential generation of $(HS-TMPA)$ and $(LS-TMPA)$ from $(HS-3MeTHF)$ and listed spectroscopic features (top). See also UV/vis (bottom) and rR difference spectra (inset). *Residual $(MeTHF)F_8Fe^{III}(O_2^{\bullet-})$ (<5%). See the SI.

peroxo complex $[(DCHIm)(F_8)Fe^{III}-(O_2^{2-})-Cu^{II}(TMPA)]^+$, $(LS-TMPA)$, analogous to those found for $(LS-AN)$ and the previously characterized $(HS-AN)/(LS-AN)$ pair.⁹ 2H NMR spectroscopy confirmed the spin change from $(HS-TMPA)$ (pyrrole signal at 99 ppm) to $(LS-TMPA)$ (pyrrole signal at 5 ppm; see SI). Resonance Raman spectroscopic characterization was also in agreement with these findings (Figure 3). While $(HS-TMPA)$ exhibited O-O, Fe-O, and Cu-O vibrations at 804, 538, and 516 cm^{-1} (shifting to 761, 516, and 491 cm^{-1} in $^{18}O_2$ samples), respectively, coordination of DCHIm to generate the complex $(LS-TMPA)$ produced three new isotope-sensitive peaks: an O-O vibration at 812 cm^{-1} ($\Delta(^{18}O_2) = 50$ cm^{-1}), an Fe-O stretch at 623 cm^{-1} ($\Delta(^{18}O_2) = 27$ cm^{-1}), and a Cu-O stretch at 533 cm^{-1} ($\Delta(^{18}O_2) = 24$ cm^{-1}). To our knowledge, this is the first case in which the effect of changing the spin state on all of the most relevant vibrations, O-O, Fe-O, and Cu-O, could be evaluated.^{14b} Moreover, the methodology used herein (i.e., low temperatures, “naked” synthon approach) leads to the clean generation of $(LS-TMPA)$ where previous attempts were unsuccessful.¹⁰

Interestingly, simple monodentate donors such as imidazoles, the actual CcO ligands, can be added to the solvato “naked” complex $(HS-3MeTHF)$ to generate new LS heme- $(O_2^{2-})-Cu$ complexes (Figure 4).¹⁵ From UV/vis spectroscopic monitoring at -125 °C, the addition of various quantities of DCHIm to the “naked” compound led to the formation of low-energy bands (741, 776, and 980 nm), analogous to the changes observed in the formation of the LS compound, $(LS-AN)$.⁹ Titration experiments showed a maximum formation of this new species at 4 equiv of DCHIm (-125 °C), suggesting a LS compound with one imidazole acting as axial ligand and the other three surrounding the Cu(II) center, thus producing $[(DCHIm)F_8Fe^{III}-(O_2^{2-})-Cu^{II}(DCHIm)_3]^+$, $(LS-3DCHIm)$. 2H NMR characterization of this complex revealed a pyrrole

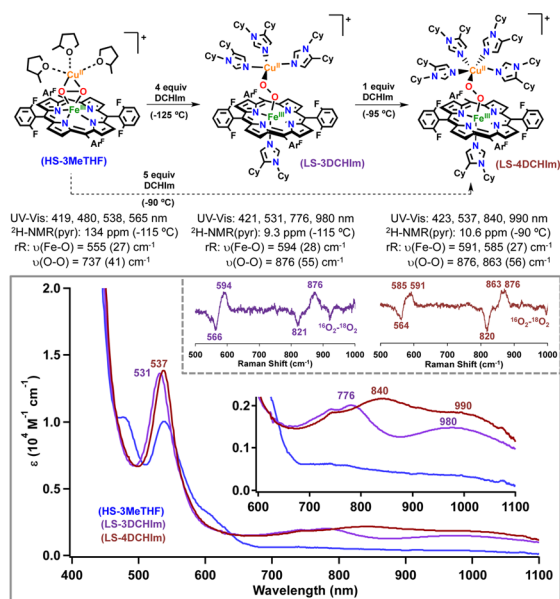


Figure 4. Sequential generation of (LS-3DCHIm) and (LS-4DCHIm) from (HS-3MeTHF) and listed spectroscopic features. See also UV/vis (bottom) and rR difference spectra (inset) along with the SI.

signal in the diamagnetic region (9.3 ppm, -115 °C), corroborating the LS ground state ($S = 0$) assignment (see SI). Further confirmation of the spin state of (LS-3DCHIm) was provided by the porphyrin ν_2 vibration observed at 1572 cm^{-1} , typical of LS Fe(III).¹⁰ Additional structural insights were provided by rR data. Laser excitation at 413 nm showed two sets of isotope-sensitive peaks, corresponding to an unusually high O-O stretching frequency at 876 cm^{-1} ($\Delta^{18}\text{O}_2 = 55$ cm^{-1}) and an Fe-O vibration at 594 cm^{-1} ($\Delta^{18}\text{O}_2 = 28$ cm^{-1}).¹⁰

Intriguing reactivity was observed for (LS-3DCHIm) when it was warmed from -125 to -90 °C. While no spectral changes occurred up to -100 °C, when the temperature reached -95 °C, small but significant shifts occurred in both the Q-band (531–537 nm) and the low-energy bands (776–840 and 980–990 nm), indicating formation of a new LS species (Figure 4). The same compound could also be generated directly at -90 °C from the “naked” compound (HS-3MeTHF) by addition of DCHIm, requiring 5 equiv for its full formation. Titration data suggest that four imidazole molecules are now bound to the Cu ion [(DCHIm) $\text{F}_8\text{Fe}^{\text{III}}(\text{O}_2^{2-})\text{-Cu}^{\text{II}}(\text{DCHIm})_4$] $^+$, (LS-4DCHIm). Cooling the (LS-4DCHIm) species to -125 °C did not lead to the reversible formation of complex (LS-3DCHIm), indicating that species (LS-4DCHIm) is the thermodynamic product formed following the generation of the kinetic product (LS-3DCHIm) at lower temperatures (-125 to -100 °C). The new species (LS-4DCHIm) exhibited a pyrrole signal at 10.6 ppm, observed by ^2H NMR at -90 °C, confirming the formulation of (LS-4DCHIm) as an antiferromagnetically coupled LS complex ($S = 0$) (see SI). The pyrrole signal was shifted compared to that of complex (LS-3DCHIm) (9.2 ppm), confirming that (LS-4DCHIm) was in fact a different LS heme-(O_2^{2-})-Cu complex. Resonance Raman experiments revealed O-O and Fe-O frequencies for (LS-4DCHIm) that were distinctive but surprisingly similar to those of (LS-3DCHIm), suggesting that coordination of an extra imidazole did not induce dramatic changes in the Fe-O and O-O bond strengths. Despite these spectral similarities,

clear differences were observed in the heme vibrations upon 413 nm excitations as well as an increase in resonance enhancement at lower energy (800–850 nm) excitation for (LS-4DCHIm). In particular, the feature assigned as the Fe-O stretch was strongly enhanced when exciting into these lower energies, identifying the 840 nm absorption band as a $\text{O}_2^{2-} \rightarrow \text{Fe}^{3+}$ charge-transfer transition (the splitting of the Fe-O and O-O vibrations for (LS-4DCHIm) is due to Fermi resonance; see SI).^{9,10}

Interestingly, the compounds (LS-3DCHIm) and (LS-4DCHIm) can also be used as starting material for the generation of other LS compounds. Addition of 1 equiv of TMPA to (LS-3DCHIm) leads to UV/vis spectral changes in both the Q-band (531–533 nm) and lower energy bands, giving the same spectrum as was generated via addition of DCHIm to the complex (HS-TMPA). We postulate that the considerable chelating ability of TMPA leads to replacement of DCHIm ligands surrounding the Cu(II) in (LS-3DCHIm) and (LS-4DCHIm), generating the more thermodynamically stable (LS-TMPA). We envision the use of (LS-3DCHIm) and (LS-4DCHIm) as starting synthons for the synthesis of a wide array of LS heme-(O_2^{2-})-Cu complexes by simple ligand addition.

To further understand the spectral differences observed in terms of the ground electronic state, we turned to DFT calculations to predict the structural and vibrational characteristics of the compounds studied. Previous work demonstrated that this method could effectively predict the spin state and Fe-O, O-O, and Cu-O vibrations, along with the electronic transitions of the (HS-AN)/(LS-AN) Fe-(O_2^{2-})-Cu complexes.^{9b} Applying this approach to (HS-TMPA)/(LS-TMPA), for which the ligand coordination around Cu is well defined (Figure 5), we first obtained optimized structures of both

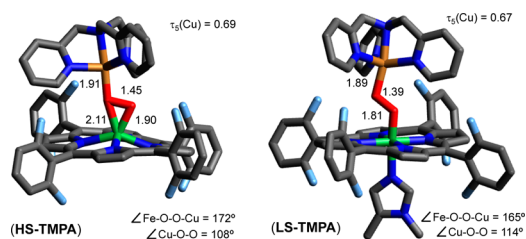


Figure 5. DFT optimized structures for (HS-TMPA) and (LS-TMPA).

complexes and confirmed that our geometry optimization of (HS-TMPA) was consistent with previous reports.^{8b} Similar to the (HS-AN)/(LS-AN) pair,⁹ which has also been recalculated here using the current methodology (see SI), addition of an axial DCHIm induced isomerization of the Fe-($\mu\text{-}\eta^2\text{-}\eta^1\text{-O}_2^{2-}$)-Cu, (HS-TMPA), to an end-on Fe-($\mu\text{-}\eta^1\text{-}\eta^1\text{-O}_2^{2-}$)-Cu structure, (LS-TMPA), leading to the observed change in spin state. This resulted in a significant reorganization of the peroxo core, as evidenced by the increased Fe-Cu distance and shortened Fe-O, O-O, and Cu-O bond lengths. The change in $d(\text{Fe-O})$ and $d(\text{Cu-O})$ can be explained by the transition to an end-on geometry in which Fe binds only one oxygen atom and the LS nature of heme-Fe(III). Although the change in $d(\text{O-O})$ is substantially smaller, it can be understood in terms of increased $\text{O}_2^{2-}(\pi^*)$ donation into the empty Fe(d_z^2) orbital, thus increasing the peroxo bond strength.

Analytical frequency calculations performed using B3LYP on (HS-TMPA) and (LS-TMPA) predicted energies and changes

in the oxygen-containing vibrational modes that are in agreement with those observed via rR spectroscopy. Moreover, the calculations reproduce reasonably the magnitude of changes observed, showing that the spin change has a profound impact on the Fe-O vibration ($\Delta\nu(\text{Fe-O}) = 85$ (expt) and 106 cm^{-1} (calcd)) but a small effect on the O-O ($\Delta\nu(\text{O-O}) = 8$ (expt) and 9 cm^{-1} (calcd)) and Cu-O vibrations ($\Delta\nu(\text{Cu-O}) = 17$ (expt) and 33 cm^{-1} (calcd)). Overall, the most pronounced effect of the (HS-TMPA)/(LS-TMPA) spin change was the increase in the Fe-O bond strength, which is expected given the change in spin state and the peroxo binding mode. Interestingly, these trends correlate well with the previous (HS-AN)/(LS-AN) results, especially the effect of the Fe-(O₂²⁻) binding mode (η^2 to η^1) on observed core vibrations.^{9b} Strikingly, although both (LS-AN) and (LS-TMPA) possess end-on peroxo cores, substantial differences in the Cu geometry were found (i.e., Cu-O-O angle, τ value; see SI); thus, the overall Fe-(O₂²⁻)-Cu structural and spectroscopic properties vary significantly.¹⁶ The unique plasticity shown by the Fe-(O₂²⁻)-Cu cores reported herein leads us to postulate that a similar bridging peroxo intermediate could form during the catalytic cycle of CcO, prior to the O-O cleaving step.¹⁷

In conclusion, we have demonstrated the versatility of the “naked” compound (HS-3MeTHF) as a starting point for the generation of heme-peroxo-Cu cores with different coordination environments and spin states. The approach is general and broadly applicable, as will be reported elsewhere. Overall, our results indicate that subtle changes in the ligand environment surrounding the Cu(II) center (i.e., geometry and/or electronics) affect the overall structure of the Fe-(O₂²⁻)-Cu systems, elongating (weakening) or shortening (strengthening) the Fe-O, O-O, and Cu-O distances along with substantially varying the core angles. Our ongoing studies are focused on investigating whether these structural differences translate into differing chemical behavior; a key approach will be to evaluate the reductive O-O cleavage chemistry of these heme-(O₂²⁻)-Cu complexes by employing systematically varied H⁺/e⁻ sources (pK_a/E^0). Such investigations will likely provide fundamental insights into the intriguing and critically important $4\text{H}^+/4\text{e}^-$ O₂ reduction process occurring in chemical systems (e.g., fuel cells) and biological oxidases such as CcO.

■ ASSOCIATED CONTENT

● Supporting Information

Figures S1–S17, Scheme S1, and Tables S1–S5. This material is available free of charge via the Internet at <http://pubs.acs.org>.

■ AUTHOR INFORMATION

Corresponding Authors

edward.solomon@stanford.edu
karlin@jhu.edu

Notes

The authors declare no competing financial interest.

■ ACKNOWLEDGMENTS

This research was supported by the U.S. NIH (GM60353 to K.D.K. and DK31450 to E.I.S.). I.G.-B. thanks the European Commission for a Marie Curie IOF Fellowship.

■ REFERENCES

- (1) Ray, K.; Pfaff, F. F.; Wang, B.; Nam, W. *J. Am. Chem. Soc.* **2014**, *136*, 13942.
- (2) (a) Fukuzumi, S.; Yamada, Y.; Karlin, K. D. *Electrochim. Acta* **2012**, *82*, 493. (b) Cracknell, J. A.; Vincent, K. A.; Armstrong, F. A. *Chem. Rev.* **2008**, *108*, 2439. (c) Su, D. S.; Sun, G. *Angew. Chem., Int. Ed.* **2011**, *50*, 11570.
- (3) (a) Ortiz de Montellano, P. R. *Chem. Rev.* **2010**, *110*, 932. (b) Kim, E.; Chufán, E. E.; Kamaraj, K.; Karlin, K. D. *Chem. Rev.* **2004**, *104*, 1077.
- (4) (a) Momenteau, M.; Reed, C. A. *Chem. Rev.* **1994**, *94*, 659. (b) Traylor, T. G.; Traylor, P. S. In *Active Oxygen: Active Oxygen in Biochemistry*; Valentine, J. S., Foote, C. S., Greenberg, A., Liebman, J. F., Eds.; Chapman & Hall: New York, 1995; p 84.
- (5) (a) Hatcher, L. Q.; Karlin, K. D. *J. Biol. Inorg. Chem.* **2004**, *9*, 669. (b) Lewis, E. A.; Tolman, W. B. *Chem. Rev.* **2004**, *104*, 1047. (c) Mirica, L. M.; Ottenwaelder, X.; Stack, T. D. P. *Chem. Rev.* **2004**, *104*, 1013.
- (6) Warren, J. J.; Tronic, T. A.; Mayer, J. M. *Chem. Rev.* **2010**, *110*, 6961.
- (7) Chufán, E. E.; Puiui, S. C.; Karlin, K. D. *Acc. Chem. Res.* **2007**, *40*, 563.
- (8) (a) Ghiladi, R. A.; Hatwell, K. R.; Karlin, K. D.; Huang, H.-w.; Moënne-Loccoz, P.; Krebs, C.; Huynh, B. H.; Marzilli, L. A.; Cotter, R. J.; Kaderli, S.; Zuberbühler, A. D. *J. Am. Chem. Soc.* **2001**, *123*, 6183. (b) del Rio, D.; Sarangi, R.; Chufán, E. E.; Karlin, K. D.; Hedman, B.; Hodgson, K. O.; Solomon, E. I. *J. Am. Chem. Soc.* **2005**, *127*, 11969. (c) Chufán, E. E.; Mondal, B.; Gandhi, T.; Kim, E.; Rubie, N. D.; Moënne-Loccoz, P.; Karlin, K. D. *Inorg. Chem.* **2007**, *46*, 6382.
- (9) (a) Kieber-Emmons, M. T.; Qayyum, M. F.; Li, Y.; Halime, Z.; Hodgson, K. O.; Hedman, B.; Karlin, K. D.; Solomon, E. I. *Angew. Chem., Int. Ed.* **2012**, *51*, 168. (b) Kieber-Emmons, M. T.; Li, Y.; Halime, Z.; Karlin, K. D.; Solomon, E. I. *Inorg. Chem.* **2011**, *50*, 11777.
- (10) Halime, Z.; Kieber-Emmons, M. T.; Qayyum, M. F.; Mondal, B.; Gandhi, T.; Puiui, S. C.; Chufán, E. E.; Sarjeant, A. A. N.; Hodgson, K. O.; Hedman, B.; Solomon, E. I.; Karlin, K. D. *Inorg. Chem.* **2010**, *49*, 3629. For the (LS-3DCHIm) and (LS-4DCHIm) complexes, no resonance enhancement of the Cu-O vibrations was observed. The ν_2 and ν_4 values for the HS/LS heme-peroxide-copper complexes described herein are summarized in Table S1.
- (11) Ghiladi, R. A.; Kretzer, R. M.; Guzei, I.; Rheingold, A. L.; Neuhold, Y.-M.; Hatwell, K. R.; Zuberbühler, A. D.; Karlin, K. D. *Inorg. Chem.* **2001**, *40*, 5754.
- (12) Kim, E.; Helton, M. E.; Wasser, I. M.; Karlin, K. D.; Lu, S.; Huang, H.-w.; Moënne-Loccoz, P.; Incarvito, C. D.; Rheingold, A. L.; Honecker, M.; Kaderli, S.; Zuberbühler, A. D. *Proc. Natl. Acad. Sci. U.S.A.* **2003**, *100*, 3623.
- (13) Three solvent molecules are proposed to surround the Cu center in the “naked” complex (HS-3MeTHF) due to its spectroscopic similarity with other well-characterized side-on heme-(O₂²⁻)-Cu systems with tridentate ligands surrounding the Cu ion.^{7,8c,12}
- (14) (a) Ohta, T.; Liu, J.-G.; Naruta, Y. *Coord. Chem. Rev.* **2013**, *257*, 407. (b) Liu, J. G.; Naruta, Y.; Tani, F. *Angew. Chem., Int. Ed.* **2005**, *44*, 1836. Naruta and co-workers observed similar behavior in their related heme-copper binuclear compounds, where coordination of a tethered imidazole caused a small change in the O-O vibration (HS = 799 cm^{-1} ; LS = 803 cm^{-1}) with a concomitant appearance of an Fe-O vibration at high energies (611 cm^{-1}).
- (15) Citek, C.; Lyons, C. T.; Wasinger, E. C.; Stack, T. D. P. *Nat. Chem.* **2012**, *4*, 317.
- (16) DFT calculations to gain insights into the structural and electronic properties of the (HS-3MeTHF), (LS-3DCHIm), and (LS-4DCHIm) complexes are currently in progress.
- (17) (a) Fee, J. A.; Case, D. A.; Noodleman, L. *J. Am. Chem. Soc.* **2008**, *130*, 15002. (b) Du, W.-G. H.; Noodleman, L. *Inorg. Chem.* **2013**, *52*, 14072. (c) Blomberg, M. R. A.; Siegbahn, P. E. M.; Wikström, M. *Inorg. Chem.* **2003**, *42*, 5231. (d) Muramoto, K.; Ohta, K.; Shinzawa-Itoh, K.; Kanda, K.; Taniguchi, M.; Nabekura, H.; Yamashita, E.; Tsukihara, T.; Yoshikawa, S. *Proc. Natl. Acad. Sci. U.S.A.* **2010**, *107*, 7740.